View Article Online / Journal Homepage / Table of Contents for this issue
Dynamic Article Links

Lab on a Chip

Cite this: *Lab Chip*, 2011, **11**, 788

www.rsc.org/loc

TUTORIAL REVIEW

Published on 08 February 2011. Downloaded by Ecole Sup de Physique et de Chimie Industrie on 30/09/2014 09:43:27.

Microfluidics and complex fluids†

Ph Nghe,[a] E. Terriac,[a] M. Schneider,[a] Z. Z. Li,[a] M. Cloitre,[b] B. Abecassis[a] and P. Tabeling*[a]

Received 12th July 2010, Accepted 12th January 2011
DOI: 10.1039/c0lc00192a

In this paper, we describe four experimental studies we carried out over the last four years in the MMN lab, regarding the dynamical behaviour of complex fluids in microfluidic systems. The topics are: (1) Polymer breakup in microfluidic systems. (2) Flows of polymer solutions in microchannels close to a smooth wall. (3) Shear banding flows in microchannels (rheology, instabilities). (4) Flows of concentrated solutions of microgel particles through microchannels. Depending on the situation, we exploit the duality low Reynolds numbers/high Weissenberg numbers (for instance, by working at high shear rates without generating turbulence), use visualization windows naturally offered by the microfluidic environment or take advantage of the integration of various functionalities on the chip. In all cases, new information, hardly accessible to non-miniaturized approaches, could be obtained by using microfluidic technology.

Introduction

Complex fluids are omnipresent, and in the short history of microfluidics, they naturally came into play at different levels, often in a crucial way. This feature is illustrated by Fig. 1, which represents a microfluidic device microfabricated in the Microfluidic lab of ESPCI.[1] The system is a regular lattice of 20 000 individual channels ($80 \times 80 \times 220\ \mu m^3$) forming a network that mimicks the structure of porous media. The system is made in PDMS (polydimethylsiloxane) and part of the network has been coated with PAA (polyacrylicacid) (see Fig. 1a). PDMS is hydrophobic and PAA hydrophilic so that the wetting properties of this network are indeed heterogeneous. In Fig. 1b, the system was initially filled with water and the experiment consisted of injecting red oil with a syringe pump into the network, pushing water gently out of the microfluidic chip.

[a]*MMN, ESPCI, Gulliver CNRS, 10 rue Vauquelin, 75005 Paris, France; Web: www.mmn.espci.fr*
[b]*MMC, ESPCI, 10 rue Vauquelin, 75005 Paris, France*
† Published as part of a LOC themed issue dedicated to French Research: Guest Editor Professor Jean-Louis Viovy.

P. Tabeling

Patrick Tabeling has been leader of the group MMN (Microfluidics MEMS and Nanostructures) since 2001. He has occupied various positions in different laboratories: Visiting researcher in Chicago University (1984–1985), Chargé/Directeur de Recherches CNRS in the Department of Physics in ENS (1985–2001), visiting professor to UCLA, and is now Directeur de Recherches/Professor at ESPCI. He was professor chargé de cours at the Ecole Polytechnique (1996–2008) He is the author of 191 papers (114 in refereed journals), 9 patents (3100 citations, h factor 33), 65 invited talks in international conferences; he is divisional editor of Physical Review Letters, Associate Editor of Physics of Fluids and Biomicrofluidics, guest editor of CRAS and PNAS. He published the book entitled "An introduction to microfluidics" (Oxford University Press – a french version being edited by Belin) in 2005.

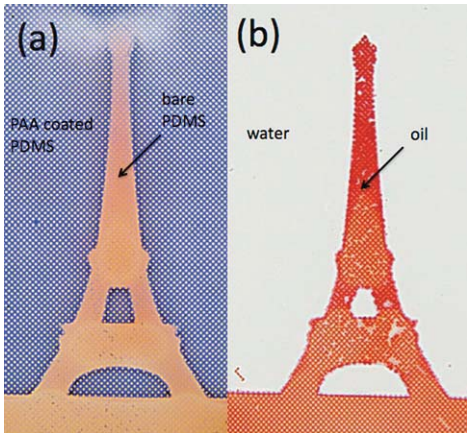

Fig. 1 (a) Network system containing a regular lattice of 20 000 individual channels ($80 \times 80 \times 220\ \mu m^3$) where an area (in blue) outlining the Eiffel tower was subjected to hydrophilic treatment. The height of the Eiffel Tower is 2 cm (b) Oil (red) injected into the network does not enter the hydrophilicly treated channels hence revealing the contours of the treated area.

This journal is © The Royal Society of Chemistry 2011

View Article Online

Published on 08 February 2011. Downloaded by Ecole Sup de Physique et de Chimie Industrie on 30/09/2014 09:43:27.

One observes, as expected, that oil (colored in red) moves into the hydrophobic (lipophilic) zones, pushing water forward, and does not penetrate into the hydrophilic zones where water stays.[1] Eventually, one gets in red (oil) and white (water) the Eiffel tower pattern of Fig. 1a imposed by the mask used in the photo-patterning technique.

This experiment illustrates that in the domain of microfluidics, complex fluids come into play at three levels:

• At the microfabrication level: PDMS is a polymer melt that is cured to produce the solid substrate forming the chip material.[2]

• At the surface level, on which acrylic acid has been polymerized *in situ*.

• At the operating level where complex fluids such as polymer melts, are currently used as working fluids (although in the present experiment, we used mineral oil).

There are thus a number of circumstances through which complex fluids and microfluidics interact. The topics are vast and here, we will restrict ourselves to the dynamical facets of the subject. In this area, several examples illustrate valuable couplings between microfluidic technology and complex fluid dynamics:

• Microfluidic technology played a key role in the early single molecule experiments, by finely controlling the elongationnal flow that develops around beads grafted with DNA strands.[3] The same technology has been used in a number of single molecule studies.[4]

• Non-linear behavior of polyacrylamide solutions was used to realize novel actuators including no moving parts.[5]

• New instabilities of flows of polymer solutions through restrictions have been observed.[6]

• Microfluidic technology has been used to invent new rheometers.[7,8] This approach led to determine for the first time the rheology of wormlike micelle solutions at high shear rates,[8,9] and provide information on the rheological behavior of DNA solutions.[10,11]

All these experiments or devices benefited from low Reynolds number conditions, where the regimes are laminar and consequently the flow can be kept under remarkable control.[2] In the meantime, important deformation rates can be achieved, giving rise to rich dynamics. This crucial remark (outlined in ref. 12), can be formalized in the following way: for a polymer solution, one may define the Reynolds Re and the Weissenberg numbers Wi (along with their ratio, the Elasticity number E) by the expressions:

$$Re = \frac{\rho \dot{\varepsilon} l^2}{\mu} \; Wi = \dot{\varepsilon}\tau \; E = \frac{Wi}{Re} = \frac{\mu\tau}{\rho l^2} \qquad (1)$$

in which ρ is the fluid density, $\dot{\varepsilon}$ the deformation rate (equal to the shear rate in a pure shear flow, the elongationnal or strain rate in a pure elongationnal flow), μ the dynamic viscosity, and τ the relaxation constant of the polymer. The Weissenberg number expresses how much polymer chains stretch out when subjected to an imposed deformation rate. At low Wi, the flow adopts a newtonian behavior and it would be difficult to detect, from the inspection of the friction exerted by the fluid onto the walls, that polymers have been added to the solution. At large Wi, polymers undergo conformational changes that affect the flow behaviour. In ordinary size systems, and with the current polymer solutions that are used, there is no possibility to obtain large Wi and in the meantime small Re. According to (1), their ratio $E = Wi/Re$ is typically small and consequently, large Wi implies large Re. As we move to micrometric systems, the elasticity number E considerably increases, reaching several order of magnitude. Therefore, one may obtain large Wi and in the meantime small Re in those systems.

In this paper we show several examples where complex fluids and microfluidic technology combine in an interesting way, substantiating the precedent remarks. In the spirit of the 10th Anniversary France issue of *Lab on a Chip*, we will describe the work done in that area in the Microfluidic lab of ESPCI over the last couple of years. The paper is not intended to be a research paper, but rather a *Tutorial Review* in which we outline interesting combinations between complex fluids and microfluidics. In some cases, we mention preliminary results. In other cases, the material has already been published and the reader may find detailed information in ref. 1, 9, 20, 28 and 32. The topics we will develop here are thus the following:

• Polymer breakup in microfluidic systems.

• Flows of polymer solutions in microchannels close to the wall.

• Shear banding flows in microchannels (microrheology, instabilities).

• Flow of concentrated solutions of microgel particles through microchannels.

Polymer breakup in microfluidic restrictions

Polymers subjected to large elongational rates stretch out and may eventually break up. This remark has considerable practical consequences in the oil industry where long chain polymers are commonly used as viscosity enhancers for blasting off oil recovery rates. Chain breakup, which leads to a reduction of the viscosity of the solution in which they are added, represents a limiting factor for this approach. There is therefore, in this domain, a need for characterizing the conditions under which polymer chains may break up, so as to design formulations increasing oil recovery rates efficiently.

The breakup problem is easy to conceptualize but difficult to investigate experimentally under well controlled conditions. All experiments performed thus far on the subject, attempting to determine critical deformation rates that would characterize breakup conditions, have been carried out under turbulent conditions.[13–18] With turbulence, the theoretical interpretation of these observations is particularly delicate and measurements obtained during decades of efforts have long appeared desperately inconsistent. By taking turbulence into account, in a subtle way, it has been possible recently to offer a consistent representation of the data,[19] but still turbulence is there and seriously complicates the analysis.

In the Microfluidics lab of ESPCI, we succeeded in building a microfluidic chip dedicated to screen polymer breakup conditions under *laminar* conditions.[20] As discussed above, miniaturization is the only pathway along which exceedingly large elongation rates and laminar regimes can coexist and this idea is somehow substantiated by the chip shown in Fig. 2.

The system includes a 70 μm high micro-fabricated planar constriction with an abrupt entry and a progressive exit. The constriction entry goes from a 500 μm wide channel to a 20 μm wide canyon-like rectangle. In this geometry, the flow created has

Published on 08 February 2011. Downloaded by Ecole Sup de Physique et de Chimie Industrie on 30/09/2014 09:43:27.

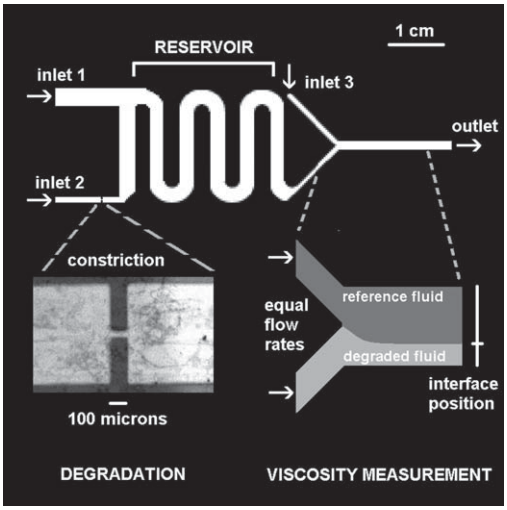

Fig. 2 Integrating a polymer degradation step and a viscosity measurement step on a microchip leads to a 40-fold increase of the measurement rate, compared to using conventional rheometers. In the degradation zone, polymer solutions are submitted to high deformation rates by flowing through a constriction, eventually leading to their breakage under mechanical stress. The viscosimeter is based on detection of the displacement of the interface between the solution under study and a reference fluid. The reservoir and an external valve ensure decoupling between the two steps.

a strong extensional component in the direction of the flow located in the accelerating zone located just before the constriction. Inside the constriction, the polymer solution is mainly submitted to shear and the progressive exit minimizes a second strong extensional event in the width direction generated by the expansion. The characteristic elongation rate at the entry of the constriction equals the shear rate in the constriction which is the maximum deformation rate imposed on the polymers in the flow, referred as $\dot{\varepsilon}_d$. We deduce $\dot{\varepsilon}_d$ from the imposed flow rate Q, considering the maximum shear rate in the Poiseuille flow between two parallel planes, given the aspect ratio of the canyon like constriction. This estimate leads to the following relation:

$$\dot{\varepsilon}_d = \frac{6\ Q}{w^2 h} \tag{3}$$

with $h = 60$ μm the height of the constriction and $w = 20$ μm the width. Given the contraction ratio, the shear rates imposed on the fluid outside the the constriction zone are 75 times lower than $\dot{\varepsilon}_d$, so that polymer degradation occurs only in the constriction zone over a wide range of imposed flow rates.

To be able to degrade short chains, one has to operate with large deformation rates and consequently large pressure drops along the microsystems. The system is therefore molded in a hard material (photocurable glue (NOA 81)) from a PDMS master.[14] As indicated in ref. 21, no deformation or leakage is observed up to 15 bars. In practice, due to pressure resistance limitations, a maximum of $\dot{\varepsilon}_d = 10^7\ s^{-1}$can be reached.

After the chains pass through the constriction, viscosity is measured on-chip, using a comparator and a reference fluid. If the reference fluid is of viscosity η_1 and the fluid under study of viscosity η_2 and the flow-rate is the same for both fluids, it can be shown[22] that

$$\frac{\eta_1}{\eta_2} = \frac{w_1}{w_2}, \tag{4}$$

with w_1 and w_2 the respective widths occupied by the reference fluid and the studied fluid. We use as a reference fluid the non-degraded polymer solution so that the position of the interface is directly linked to the viscosity ratio between the degraded and the non-degraded polymer solution.

The collection of results we obtained in this system is summarized in Fig. 3, in which the deformation rate is rescaled so as to optimize data collapse. Based on a rough optimization of data collapse, we determined the following empirical law for the critical shear rate

$$\dot{\varepsilon}_c = (M_w/M_0)^{-1.7}(c/c_0)^{-0.7} \tag{5}$$

where M_w is the molar mass of the polymer, c the concentration, and M_0 and c_0 fitting parameters. Theoretical considerations lead to an exponent equal to -2 for the molecular weight dependence. We are not far from this expectation. The exponent associated to the concentration c is not understood.[2]

To conclude this section, one may stress that the empirical law we found for the critical elongational rate at breakup has been obtained under laminar conditions, the Reynolds number being kept below 100. This is the first time that such well controlled conditions could be achieved. Incidentally, we also found that microfluidic technology allows to perform measurements at unprecedented speeds. Therefore, the chip we made can also be used as an instrument to screen polymer degradation, a task which is not feasible, in practice, by current technologies owing to the time it would take to obtain relevant data, associated to inherent difficulties of interpretation.

How do polymer solutions flow along smooth walls?

How do polymers flow along the walls? Do they slip? The question traces back to De Gennes's pioneering papers written in the late seventies. Thus far, the question has been investigated essentially for the case of polymer melts. De Gennes's original predictions suggested considerable slippage against the wall, with slip lengths on the order of millimetres for long chains.[23] Detailed experimental studies carried out in the nineties revealed the

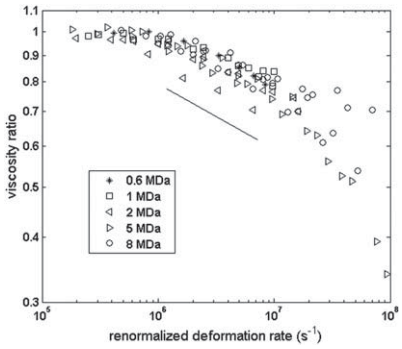

Fig. 3 Viscosity ratio of the working to the reference fluid *versus* a renormalized imposed deformation rate for PEO, with 5 different molecular weights and 5 different concentrations; the renormalization factor is devised to optimize data collapse on a single curve.

This journal is © The Royal Society of Chemistry 2011

Published on 08 February 2011. Downloaded by Ecole Sup de Physique et de Chimie Industrie on 30/09/2014 09:43:27.

crucial role of polymer adsorption at the wall and proposed a more complicated picture.[24,25] These experiments showed that at small shear rates, the polymer chains located next to the wall stick to the absorbed layer, and slippage is suppressed. At larger shear rates the chains randomly disentangle from the chains adsorbed at the wall and in such conditions, slippage arises in a way reminiscent of De Gennes's original scenario.

Much less is known for the case of polymer solutions, where depletion or enrichment of the solution close to the walls may obviously interfere with the stick–slip picture mentioned precedently.[26,27] The work we present here aims at making progress on the subject, by determining velocity profiles close to the walls at scales below the gyration radius. The results are still in a preliminary stage. In the microfluidic experiment we present here, the presence of visualization windows allows the implementation of sophisticated optical techniques dedicated to measuring flow velocities close to the wall. In the present case, we used an evanescent wave technique,[28] and succeeded to determine for the first time velocity profiles of polymer solutions within the first 300 nm of the wall, with a resolution of 20 nm.

The system is shown in Fig. 4. Briefly we collimate a laser beam through a high numerical aperture objective (100×, NA = 1.46) with an incidence angle above the critical angle for total reflection. The laser beam is focused in the back focal plane of the objective with an achromatic doublet and the incidence angle is tunable by a rotating mirror in the optical path. Tracers were imaged in a field of view of 80 × 80 μm under ~50 mW illumination on an EM-CCD camera with an acquisition rate of 25 Hz in frame-transfer mode. In the Total Internal Reflection regime, the illumination power within the channel is given by $I(z) = I_0\exp(-z/L_e)$ in which z is the distance from the wall and L_e is the optical penetration length. Under our experimental conditions, L_e was varied between 150 and 400 nm. By measuring the intensity reflected by the particles seeding the flow, we can determine, within ±15 nm accuracy, the distance of each of them from the wall. In the velocimetry technique we use, we first select particles showing constant intensity during the imaging process, determine their velocity and average out over 5000 particles. As a whole, the experimental uncertainty on the velocity measurement is on the order of 10%. Velocity distributions and seeding particle diffusion coefficients are also measured.

Here we consider pressure driven flows of PEO solutions, with different concentrations, molecular weights and distributions of the chain lengths. One important parameter in this problem is the overlap concentration c^*. At low concentrations (compared to c^*), the regime is dilute and the profiles we observed are linear; as expected, they do not differ from newtonian fluids. The situation changes as c exceeds c^*. In the experiments, we operated at different pressures, chain lengths (from 800 kD to 5 MD), concentrations, using PEO commercial solutions above c^*, *i.e.* in semi-dilute regimes. In our systems, ellipsometric measurements indicate that PEO chains adsorb onto the walls, at a rate that depends on the polymer concentration.

A typical curve obtained for 3 g l^{-1} and a molecular weight of 2 MD is shown in Fig. 5. At more than 100 nm from the wall, the velocity profile is linear and the slope corresponds to that expected from standard rheological measurements. As we approach the wall by less than 100 nm, the velocity profile levels off. As compared to "bulk" rheological behaviour, there seems to be an increase of the local viscosity of the solution. The levelling off of the velocity profile close to the wall is observed with different molecular weights, different pressures and concentrations in the semi dilute regime. The interpretation of this peculiar velocity structure remains to be done; here we discuss possible origins and speculate on a possible scenario.

• The existence of a large apparent viscosity close to the wall (on a gyration radius scale), is not easy to explain. Should we assume that polymer adsorption at the wall is negligible, then a depletion of polymer concentration would take place in the near-wall region and consequently a decrease of the local viscosity would occur, in contradiction with the experiment. If we assume instead that a polymer brush is formed at the wall, as the result of chain adsorption, then an enrichment in polymers should take place near the wall – over a radius of gyration or a correlation length – and consequently an apparent viscosity increase would occur. However, in the meantime, the brush

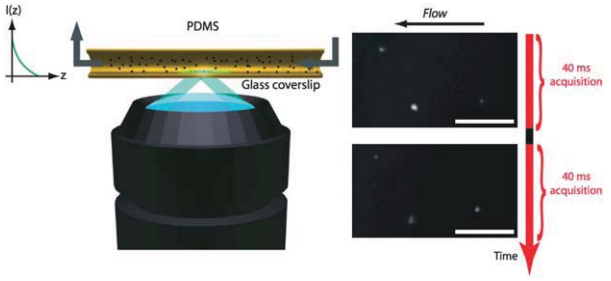

Fig. 4 (*left*) Scheme of the TIRF setup. A laser beam is collimated through a high numerical aperture objective (100×, NA = 1.46) with an incidence angle higher than the critical angle for total reflection. The laser is focused in the back focal plane of the objective with an achromatic doublet (focal length = 150 mm) and the incidence angle is tunable by a rotating mirror in the optical path. The evanescent wave created within the channel restricts fluorescence to tracers (black dots) in the vicinity of the surface. (*right*) Typical images obtained by TIRF illumination showing several fluorescent particles seeding the flow: the two images are acquired in frame-transfer mode with an exposure/acquisition time of ~40 ms. Scale bar represents 5 μm.

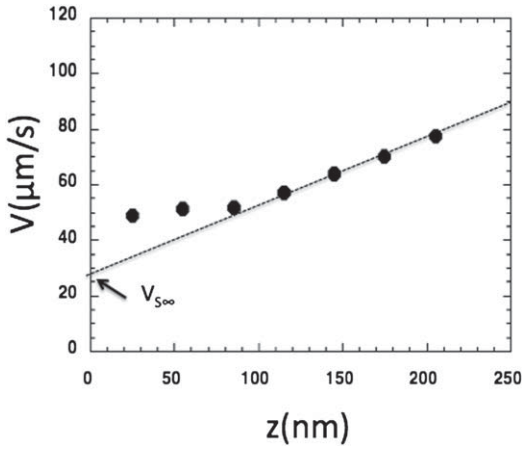

Fig. 5 Velocity profile obtained with a solution of 2 MDa PEO close to the wall, under a pressure of 50 mbar, showing the presence of a plateau region in the first tens of nanometres from the boundary condition. The (estimated) gyration radius is 50 nm in this case.

Published on 08 February 2011. Downloaded by Ecole Sup de Physique et de Chimie Industrie on 30/09/2014 09:43:27.

would suppress slippage at the wall, a feature in contradiction with the observation.

• We may speculate on a scenario that combines adsorption and dynamics. We suggest here that the apparent increase of the viscosity leading to the levelling off of the velocity close to the wall is due to the presence of stretch-recoil events. Chains adsorded to the wall stretch out under the action of the flow, desorb, recoil and are advected downstream. The conformationnal changes the chains are subjected to dissipate energy and give rise to an apparent enhancement of the viscosity, in a way similar to turbulent boundary layers seeded with polymer additives.[29] Owing to the nature of the process we discuss here, the relevant scale is the gyration radius. This scenario is compatible with the existence of a slippage at the wall. More work is obviously needed to assess the pertinence of such a scenario.

Flows of wormlike micellar solutions in microchannels

Wormlike micellar solutions are surfactant solutions well above the critical micellar concentrations. In such conditions, micelles have tube-like structures, which develop a complex dynamics still not fully understood at the moment. Rheological studies of these solutions face the difficulty that above some critical shear rate, the flow become heterogeneous, splitting into two regions, one occupying the bulk, and characterized by low shear and the other located close to the walls (the bands), associated to high shear rates and lower viscosities. An example of such flow structure is shown in Fig. 6. The appearance of this heterogeneous structure has been described in the literature as signalling the onset of an instability in the constitutive equations of these complex fluids.[30] In the meantime, in classical rheometers, dynamical instabilities develop and raise difficulties for determining the rheology of the working fluid beyond the shear banding onset.

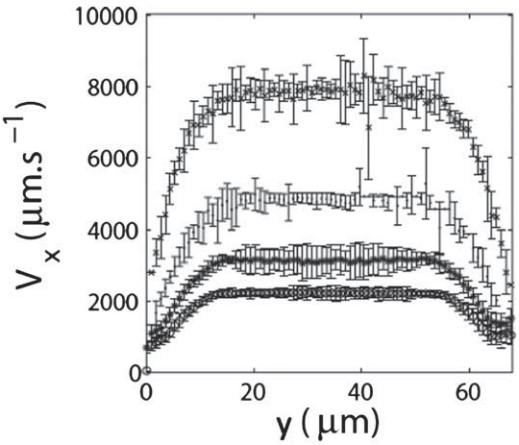

Fig. 6 Velocity profiles of wormlike micelles solutions accross the height of a rectilinear microchannel (see the coordinate system of Fig. 7), obtained at different pressures above the threshold of the onset of shear-banding at the walls. (see Ref. 9 for more information). These profiles are obtained close to the entry of the microchannel, in a region where the instabilities have small amplitudes. The plug-like aspect of these profiles is characteristic of a shear-banded Poiseuille flow: the viscosity of the solution close to the walls (where the stress is maximum) is much lower than around at the mid-height.

Working in straight microchannels and using µPIV technique[31] offers the advantage of inhibiting these dynamical instabilities and incorporating naturally the heterogeneous structure in the rheological interpretation.[7] The outcome of this approach allowed us for the first time to resolve the high shear rheological branch for the case of CTAB (CTAB 0.3M, $NaNO_3$ 0.405M).[9]

Although inhibited, the dynamical instabilities of wormlike micelle flows still develop in microchannels and this is precisely what we investigated recently in the Microfluidic Lab.[32] In order to perform the study, we devised a 3D µPIV system that allows measurement in real time the velocity throughout the fluid volume.[32] The system is shown in Fig. 7.

This system allowed to reveal shear banding instabilities that manifest as an oscillation of the boundary between the bands and the bulk (see Fig. 8).

In the framework of the Johnson Segelman diffusive model, Fielding carried out a linear perturbation analysis of the basic shear banded state, and a full numerical simulation of the shear banded flow; she obtained excellent agreement with our experiment.[32] Previous work showed that shear banded flows are unstable in the Taylor–Couette geometry, where the presence of curvature is crucial.[33] Here, there is no curvature and still instabilities develop. This shows that our experiments reveal a new instability mechanism. We suggest the mechanism is based on a discontinuity of viscoelastic properties at the interface between the bands located near the horizontal walls and the highly viscous bulk.[32]

Flows of microgel bead solutions in microchannels

Concentrated microgel beads solutions are solutions of hydrogel beads, typically 100–300 nm in size, in concentrations lying close and above the close packing.[34] These complex fluids are extensively used in the chemical industry to synthesize all sort of pastes and plastics. The transport of such beads under control is

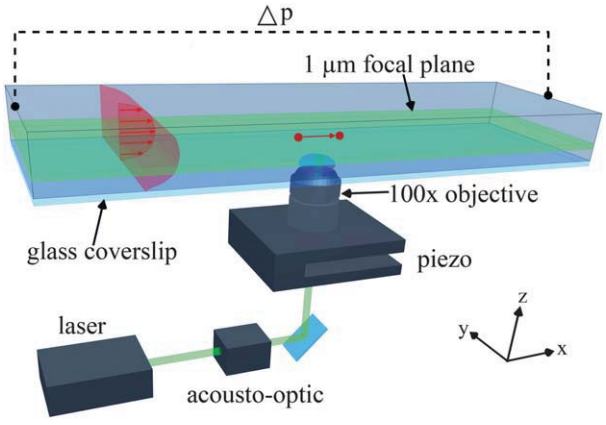

Fig. 7 Fluorescent tracers of diameter 500 nm are tracked at 50 Hz with a charged coupled device camera through a 100× oil immersion objective mounted on a piezo, giving a 1 µm thick focal plane that can be displaced in y with 10 nm resolution. Image acquisition is performed at a given (x, z) position determined by a moving table. Recorded images have a size 36 µm, 72 µm and correlations are computed on subimages of size 9 µm along z. As a whole, then, a time averaged velocity field can be imaged over the sample with spatial resolution 36 µm, 1 µm, 9 µm.

This journal is © The Royal Society of Chemistry 2011

Published on 08 February 2011. Downloaded by Ecole Sup de Physique et de Chimie Industrie on 30/09/2014 09:43:27.

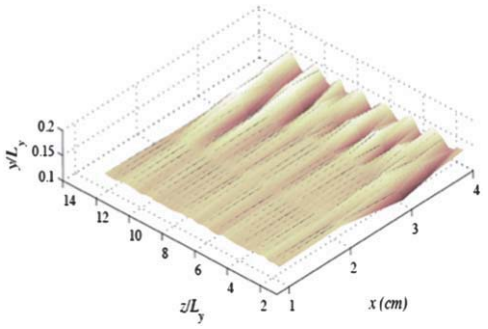

Fig. 8 Evolution of the interface at the edge of the bands of a shear-banding flow (such as the one depicted in Fig. 6), as a function of the horizontal coordinates (streamwise) x and (crossstream) z. This interface is progressively destabilized along the streamwise coordinate (x), showing an undulation with a wavevector directed along the width (z) of the channel. Quantitative agreement with theory indicates a destabilization mechanism based on discontinuity of viscoelastic properties at the interface (see ref. 32 for details).

challenging, owing to the complexity of the rheology of these systems and the limited information we have on the interaction they may develop with the pipe or channel walls. Much progress has been done in this area over the last few years[35–41] but still the structure of these flows, especially in the low speed regime (which is relevant practically) is largely unknown.

In these systems, and for smooth walls, two flow regimes can be defined:

• At small stresses, a plug flow develops with large slippage at the wall (slippage regime/solid like regime).

• As the shear stress increases further, the system undergoes fluidization and Poiseuille profiles develop, with vanishing slippage at the wall (fluidized regime).

The structure of the slippage regimes – the most important ones in practice – is still under debate. A number of authors suggest the existence of a thin fluidized layer, a few microgel beads thick,[42] that ensure the transition between the bulk and the wall, while others suggest a nanometric film within which all the velocity gradients are localized.[39] Current velocity measurement techniques were unable thus far to support either theory, owing to limitations in their spatial resolution. The method we use here solves this problem, by bringing the resolution down to 20 nm, a scale appropriate for resolving the structure of these flows down to the first layer of microgel particles.

Here we show preliminary results, which reveal the flow structure of these systems. The flows we consider are sketched in Fig. 9. A pressure drop ΔP is applied and drives microgel solutions steadily through straight microchannels. The microchannel dimensions we consider here are 16 μm high, 100 μm wide and 1.5 cm long.

The microchannels are classically created by using classical photolithography patterning process of SU8 photoresist in a clean-room environment. The photoresist is spun on a pre-cleaned silicon wafer, soft-baked, exposed with UV radiation through the mask and post-baked. The mixture is then cast against the silicon master, cured at 65 °C for 2 h then peeled off the mold. The cross linked PDMS piece is bonded against a glass plate, 170 μm thick, using an oxygen plasma, thus producing a closed microfluidic system.

The grains are formed with self cross-linked acrylate chains. Their averaged size is 250 nm with a dispersivity on the order of 400%. We added polystyrene fluorescent particles, 20 nm in diameter, in the final step of the process to seed the flow. The rheology of the microgel solutions we analyze here is measured by using a standard Couette viscosimeter (an example is shown on Fig. 1b). In the present review, we concentrate our attention on the analysis of concentrated solutions, *i.e.* whose volume fractions range between 60 and 90%. In terms of mass concentrations, we consider domains lying between 1 and 1.6%

The microgel solutions are driven through PDMS microchannels by using Fluigent pressure pumps. The pressures that we impose lie in the range 0–10 Pa and the cross-sectionally averaged flow speeds we obtained are comprised between 0 and 50 μm s^{-1}. The two techniques we used to measure the local velocities are nanoPTV (NanoParticle Tracking Velocimetry) (for distance less than 300 nm from the wall) and μPIV (micro Particle Image Velocimetry) (for distances above 1 μm from the wall).

Fig. 10 shows that under different flow conditions, *i.e.* for 100 and 250 mbar, the grain velocity is independant of its distance to the wall. This property is observed in the slippage regime (*i.e.* below the yield stress), and at different concentrations above the close packing condition. Measurements extended to the entire microchannel indicate that the velocity near the wall is also that holding in the bulk. From these measurements one may infer that in the slippage regime, *all the microgel grains* develop a pure translational motion, constant throughout the system down to 20 nm from the wall. We may suggest the existence of a lubricating film over which the grains move steadily. The expected thickness of such a film (estimated with the formula: $U \sim \frac{\sigma}{\mu U} \sim \frac{\Delta P w}{2\mu L U}$ where U, σ, μ are respectively the grain speed, the shear stress and the solution viscosity) range between 3 and 10 nm, which is

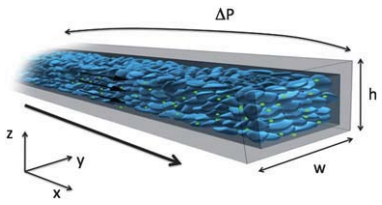

Fig. 9 Sketch of the flow we study in the review. The flow is driven with a pressure pump through a microchannel, 16 μm high, 100 μm wide and 1.5 cm long.

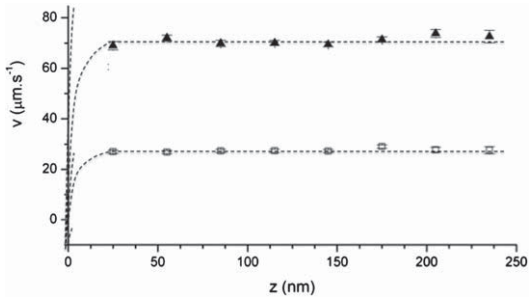

Fig. 10 Two velocity profiles obtained with nanoPTV technique, for a 1.6% microgel solution driven downstream at different pressures (from bottom to top: 100, 250 mbar).

View Article Online

Published on 08 February 2011. Downloaded by Ecole Sup de Physique et de Chimie Industrie on 30/09/2014 09:43:27.

consistent with the spatial resolution of our nanoPTV technique. Remarkably, in this regime, all the beads are driven downstream by viscous stresses localized in a nanometric layer.

Conclusion

In the present paper, we investigated four topics:

- Polymer breakup in microfluidic systems.
- Flows of polymer solutions in microchannels close to the wall.
- Shear banding flows in microchannels (rheology, instabilities).
- Flow of concentrated solutions of microgel particles through microchannels.

In all cases, the microfluidic environment offers advantages that led to obtain new information on these systems. The information we could obtain is listed below:

- Polymer breakup in microfluidic systems: measurements of the critical elongational rates under *laminar* conditions.
- Flows of polymer solutions in microchannels close to the wall: suggestion that a specific flow structure exists on the gyration radius scale (at this stage, more work is needed to draw out firm conclusions).
- Shear banding flows in microchannels: resolution of the rheology at large shear rates and discovery of new instabilities.
- Flow of concentrated solutions of microgel particles through microchannels: observation of a plug flow structure down to the subparticle scale.

In some cases, we exploited the low Reynolds numbers/high Weissenberg numbers duality. In other cases, we took advantage of the visualization windows naturally offered by the microfluidic environment (a consequence of the planar technology used to build microfluidic systems). In still other situations, the integration of several functionalities on the chip turned out to be advantageous for reaching large amounts of data.

Acknowledgements

This paper summarizes contributions made at MMN over the last few years, some of them being conducted in close collaboration with A. Ajdari. The work we report here generated exchanges with many colleagues. We warmly thank all of them. We acknowledge CNRS, TOTAL, Schlumberger, ESPCI for their financial support to this work.

Notes and references

1 M. Schneider, Y. Tranh, F. Rezgui and P. Tabeling, *Anal. Chem.*, 2010, **82**(21), 8848.
2 *Introduction to Microfluidics*, P. Tabeling, Oxford University Press, 2005.
3 T. T. Perkins, S. R. Quake, D. E. Smith and S. Chu, *Science*, 1994, **264**(5160), 822.
4 B. Ladoux, J. P. Quivy, P. Doyle, O. du Roure, G. Almouzni and J. L. Viovy, *Proc. Natl. Acad. Sci. U. S. A.*, 2000, **97**(26), 14251.
5 A. Groisman, M. Enzelberger and S. Quake, *Science*, 2003, **300**, 955.
6 L. E. Rodd, T. P. Scott, D. V. Boger, J. J. Cooper-White, G. H. McKinley, in *XIVth Int. Congr. on Rheology*, Korean Society of Rheology, Seoul, South Korea, 2004.
7 G. Degre, P. Joseph, P. Tabeling, S. Lerouge, M. Cloitre and A. Ajdari, *Appl. Phys. Lett.*, 2006, **89**, 24104.
8 C. Masselon, J. B. Salmon and A. Colin, *Phys. Rev. Lett.*, 2008, **100**, 038301.
9 P. Nghe, G. Degre, P. Tabeling and A. Ajdari, *Appl. Phys. Lett.*, 2008, **93**, 204102.
10 C. M. Shroeder, D. E. Teixera, E. S. Shaqfeh and S. Chu, *Macromolecules*, 2005, **38**, 1967.
11 R. E. Teixeira, A. K. Dambal, D. H. Richter, E. S. Shaqfeh and S. Chu, *Macromolecules*, 2007, **40**, 2461.
12 T. Squires and S. Quake, *Rev. Mod. Phys.*, 2005, **77**, 977–1026.
13 T. Q. Nguyen and H. H. Kausch, *J. Non-Newtonian Fluid Mech.*, 1988, **30**, 125.
14 T. Q. Nguyen and H. H. Kausch, *Macromolecules*, 1990, **23**, 5137.
15 J. D. Clay and K. W. Koelling, *Polym. Eng. Sci.*, 1997, **37**, 5.
16 J. A. Odell, A. Keller and Y. Rabin, *J. Chem. Phys.*, 1988, **88**, 4022.
17 J. A. Odell, A. J. Muller, K. A. Narh and A. Keller, *Macromolecules*, 1990, **23**, 3092.
18 A. J. Muller, J. A. Odell and S. Carrington, *Polymer*, 1992, **33**, 12.
19 M. T. Islam, S. A. Vanapalli and M. J. Solomon, *Macromolecules*, 2004, **37**, 1023.
20 P. Nghe, P. Tabeling and A. Ajdari, *J. Non-Newtonian Fluid Mech.*, 2010, **165**, 313.
21 D. Bartolo, G. Degre, P. Nghe and V. Studer, *Lab Chip*, 2008, **8**, 274.
22 P. Guillot, P. Panizza, J. B. Salmon, M. Joanicot and A. Colin, *Langmuir*, 2006, **22**, 6438.
23 P. G. De Gennes, *CRAS*, 1979, **B288**, 219.
24 K. B. Migler, H. Hervet and L. Leger, *Phys. Rev. Lett.*, 1993, **70**(3), 287.
25 H. Hervet and L. Leger, *CRAS*, 2003, **4**, 241.
26 L. Leibler, J. F. Joanny and P. G. De Gennes, *J. Polym. Sci.*, 1979, **17**(6), 1073.
27 Eisenriegler and R. Maassen, *J. Chem.Phys.*, 2002, **116**(1), 449.
28 C. Bouzigues, P. Tabeling and L. Bocquet, *Phys. Rev. Lett.*, 2008, **101**, 114503.
29 An example isG. Ryskin, *Phys. Rev. Lett.*, 1987, **59**(18), 2059.
30 M. E. Cates and S. M. Fielding, *Adv. Phys.*, 2006, **55**, 799.
31 P. Joseph and P. Tabeling, *Phys. Rev. E*, 2005, **71**, 035303.
32 P. Nghe, S. Fielding, P. Tabeling and A. Ajdari, *Phys. Rev. Lett.*, 2010, **104**, 248503.
33 M. A. Fardin, B. Lasne, O. Cardoso, G. Gregoire, M. Argentina, J. P. Decruppe and S. Lerouge, *Phys. Rev. Lett.*, 2009, **103**, 028302.
34 P. Coussot, *Soft Matter*, 2007, **3**, 528.
35 J. Goyon, A. Colin, G. Ovarlez, A. Ajdari and L. Bocquet, *Nature*, 2008, **454**, 84.
36 H. M. Princen, *J. Colloid Interface Sci.*, 1984, **105**, 150.
37 S. Marze, A. Saint-Jalmes and D. Langevin, *Colloids Surf., A*, 2005, **263**, 121.
38 N. D. Denkov, S. Tcholakova, K. Golemanov, K. P. Ananthapadmanabhan and A. Lips, *Phys. Rev. Lett.*, 2008, **100**, 138301.
39 P. Ballesta, R. Besseling, L. Isa, G. Petekidis and W. C. Poon, *Phys. Rev. Lett.*, 2008, **101**, 258301.
40 R. Borrega, PhD thesis, Université Pierre et Marie Curie, 2000.
41 J. R. Seth, M. Cloitre and R. T. Bonnecaze, *J. Rheol.*, 2006, **50**, 353.
42 J. R. Seth, M. Cloitre and R. T. Bonnecaze, *J. Rheol.*, 2008, **52**, 1241.

 This journal is © The Royal Society of Chemistry 2011